A Multi-Robot Hoisting System that Achieves Precision by Constructing and Exploiting Mechanical Constraints through Non-Prehensile Control

Boris Deroo[1], Wilm Decré[1,2], and Herman Bruyninckx[1,2,3]

***Abstract*— This paper describes a multi-robot solution for pick-and-place operations, that creates and exploits mechanical constraints to control the payload through interactions. The task requirements are split across a strong, but imprecise, crane and an accurate, but weak, dual-arm manipulator. First, the design of the manipulator is discussed. Its task is to align its end-effectors with features in the environment and create additional mechanical constraints. Second, a coordinated control strategy between agents is described in order to accurately position and align a payload relative to another object in the environment. The crane controller exploits interactions between the payload and the mechanical constraints created by the manipulator to control the payload and reduce its state uncertainty.**

A box stacking use case was performed to validate the method. The task could be successfully executed, even when tracking errors were superimposed on the position- and velocity setpoints of the crane control. This highlights the robustness of the approach, and the possibility to implement it on existing, imprecise cranes with low control bandwidth.

I. INTRODUCTION

In the **context** of the logistics and construction industry, plenty of pick-and-place tasks do not require high precision throughout the motion, e.g., (de)palletising, truck (un)loading, bricklaying, etc. In these examples, the payload is not fragile, and accuracy is only needed at the start and/or end of the trajectory. These types of pick-and-place tasks will be the focus of this paper.

Current solutions to automate such tasks most often use a serial robot manipulator. The required precision is typically achieved through the free-space inverse kinematic control of the robot itself. This requires stiff links, resulting in large, heavy structures, especially when heavy payloads need to be manipulated across a large workspace.

Humans, in contrast, deploy a drastically different strategy. They tend to exploit mechanical interactions to limit the control effort and to speed up the task execution. Collisions with other objects in the environment are commonly used to achieve the required precision, e.g., pushing objects together to place them next to each other. When heavy payloads need to be manipulated, hoisting systems or cranes are often used.

A **shortcoming** of cranes is that, due to the inherent flexibility of the cable, it is difficult to accurately control their end-effector and achieve the required precision during the placement of the payload. To this end, a human operator can help by directly interacting with the payload in parallel to the crane (Fig. 1). This splits the task requirements across two heterogeneous agents, each with their own responsibilities: The strong, but imprecise, crane, responsible for counteracting the gravitational force and for generating the macro movement; The weak, but accurate, human responsible for counteracting the inertial forces and performing the fine-manipulation actions. This separation lowers the overall requirements of both individual systems



Fig. 1. Human operators manipulating a payload in parallel with a crane. Mechanical constraints are exploited to achieve precision [1].

Our **Previous work** focused on the design of a gripper to autonomously grasp the handle of a payload with a crane [2]. However, the placement of the payload was not treated. The placement position for the tasks handled in this work is often right next to (or on top of) other mechanical features, such that the payload is aligned flush with them. Thus, the required placement accuracy can be achieved through physical interaction by colliding with these features. However, often the existing environment is not sufficient to reliably control and place the payload using only a crane.

A multi-robot system solution is **proposed**, inspired by the strategy used by humans. It introduces a fine-position manipulator, in addition to a crane. Its task is to orient and position the payload during its placement. The manipulator collides and braces its end-effectors against the environment to create additional mechanical constraints. Thus, extending the environment into a more desirable configuration. Through a coordinated control, the crane exploits both the constraints created by the manipulator and the environment to control the payload with physical interactions towards its placement position. The required final accuracy is achieved by pushing and sliding the payload with non-prehensile interactions.

This paper provides two **contributions**. First, it discusses

* This work was supported by the Research Foundation-Flanders (FWO) through project ELYSA (S001821N) and by Flanders Make through SBO project Sitanav.

[1] Department of Mechanical Engineering , KU Leuven, 3000 Leuven, Belgium first_name.second_name@kuleuven.be

[2] Flanders Make, 3000 Leuven, Belgium

[3] Department of Mechanical Engineering, TU Eindhoven, Eindhoven, The Netherlands

the design of the manipulator robot, and its end-effectors used to interact with (and shape) the environment. Second, it describes a coordinated control strategy between this manipulator and a crane to robustly control, orient, and position a payload with respect to an object in this environment.

To **validate** the proposed method, a use case is investigated where a beer crate is stacked on top of and aligned with another crate in the environment. This bottom crate can only provide mechanical constraints from a lower vertical position. This is also representative for the placement of the first construction block or box in a new layer of a masonry/wall building or palletising task. The object providing the environmental constraint could be respectively a lower layer of the construction blocks, or a pallet.

The extension of this use case is the placement of a full layer. Subsequent elements to be placed on this layer can also exploit the horizontal constraints of the previously placed object(s) on the same layer. As such, more constraints are available, resulting in a simpler scenario.

II. RELATED LITERATURE

Contrary to serial manipulators, cranes and other cable-based structures scale well with the workspace and the rated payload [3]. While cable-driven parallel robots can accurately control their end-effector, they require multiple winches mounted at spread out locations, limiting their ease of deployment [4]. In addition, cable-object interactions are undesirable [5], limiting the size and amount of other objects within its workspace. Thus, traditional hoisting solutions are still prevalent for most lifting applications (e.g., tower cranes on construction sites, gantry hoists in workshops).

However, the inherent flexible nature of the hoisting cable makes it difficult to accurately control their end-effector. In order to limit the end-effector sway, both feedback [6] and feedforward [7] control strategies have been proposed.

In [8], a KUKA LBR IIWA (with a rated payload of 14kg) was used to control a payload of 65kg in parallel with a crane. However, the grasping process of the (potentially swinging) payload is not discussed. The single-arm prehensile grasp also does not scale well for increasing payload dimensions. Since the high-geared transmission is rigidly connected to the payload through the grasp, the gears could easily be damaged if oscillations need to be compensated.

In contrast, locomotive robots have low gear-ratios and are backdrivable in order to withstand repeated impacts [9]. A dual-armed manipulator with similar characteristics was used in [10] to position a payload in parallel with a crane through non-prehensile actions. This method requires good perception and models to accurately control the motion of the payload with minimal input from the manipulator.

Instead of directly controlling the payload, it can also be manipulated through interactions with its environment. Sensorless, open loop control actions that exploit the environment have been used to manipulate an object and reduce its state uncertainty [11]. The environment can also be used to assist in certain grasping strategies [12], or to assist with in-hand manipulation [13]

This work uses a similar crane-manipulator architecture. But instead of directly controlling the payload with the manipulator, the manipulator creates mechanical constraints, which the crane controller can exploit.

III. FINE-POSITION MANIPULATOR

To perform the fine-manipulation actions, a Unitree Go1 quadruped robot was mechanically converted to a dual arm manipulator (Fig. 2), using the method described in [14]. This robotic agent will be referred to as *'the manipulator'*.

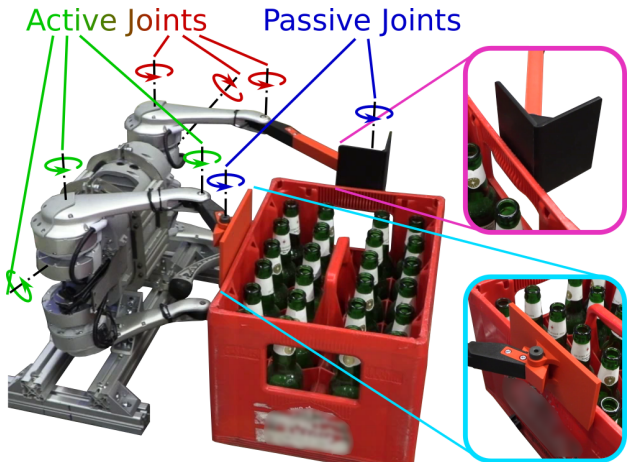


Fig. 2. Quadruped converted to a backdrivable, dual-arm manipulator. Custom end-effector are used to create mechanical constraints. Each limb has three active DoF (indicated in red, and green), and one passive DoF (indicated in blue). This allows the end-effectors to passively self-align.

The last link of both arms are exchanged for custom end-effectors, which are different for both arms. The end-effector of the right arm has a flat rectangular face (called the *'flat end-effector'* throughout the rest of the text). The one attached to the left arm has two flat, rectangular faces connected in an L-shape (the *'L end-effector'*). Their specific use for the investigated use case will be made clear in Sec. IV. An additional passive revolute joint is included between both end-effectors and the last link of their respective arm. Thus, combined with the three active DoF of each arm, both end-effectors can be moved in 3D space, and different orientations are possible in the plane of the last two joints. This allows the end-effectors to collide and passively self-align with the face of an object in the environment.

The control through mechanics principle proposed in [2] is used to guarantee proper self-alignment of the end-effector when the object is approached perpendicularly. By using this principle, only a single orientation is possible at the end of the approaching motion. Any state uncertainty on the final orientation is mechanically removed. Thus, there is no need for active actuation to control this orientation. This lowers the weight, cost, and mechanical complexity of the designed solution. The result is a passive joint that has a limited range of possible orientations (depicted for the flat end-effector in Fig. 3, the L end-effector is analogous).

The range of the end-effectors is limited from one side by the link itself, and the other side by an end stop. The

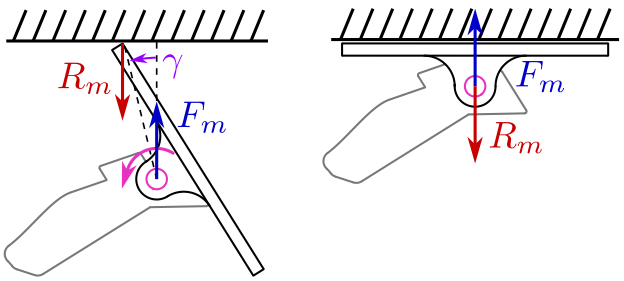


Fig. 3. Self-alignment of the flat end-effector with the environment. The offset of the reaction force R_m, caused by the manipulator force F_m, results in a rotation around the passive joint of the last link (highlighted in magenta).

resulting geometry causes the end-effector to always rotate towards the desired final orientation, regardless of its current orientation due to the moment induced by the reaction force R_m. The approaching movement can deviate up to γ from being completely perpendicular and still result in the desired behaviour. A larger value of this design parameter makes the mechanism more robust to inaccuracies on the approaching direction. This lowers the requirements of the robot control and the detection of the object. However, the trade-off is a smaller joint range and consequentially robot workspace.

The actuators use following low-level controller:

$$i = \tau + K_p e_p + K_d e_q, \tag{1}$$

with i the motor current, τ a feedforward current, e_q and e_q the error on the desired joint position and velocity, and the corresponding gains K_p and K_d. Since there is no integrating term, the joints act compliant when experiencing an external force. Due to the low gear-ratio of the actuators, variations in this force can be detected by monitoring the motor current.

IV. CONTROL STRATEGY

This section discusses the proposed control strategy used to stack a box-shaped payload on top of another box-shaped object with a crane and a dual-arm manipulator with non-prehensile, plate-shaped end-effectors.

The payload is grasped by the crane in the middle of its top-most surface. The pose of the payload is measured throughout the execution. The manipulator is positioned in front of a static box-shaped object in the environment (henceforth referred to as *'the object'*), such that its end-effectors can each reach one of the sides of the closest corner. The localisation and navigation of the manipulator itself to get to this position is out of scope for this paper. The workspace of the crane covers both the manipulator and the object. This object will be exploited in the control strategy as a mechanical constraint to align the end-effectors with.

The set of subtasks used in the stacking skill all perform mechanical alignment actions, each aligning different features of the payload, the object, and the manipulator (Fig. 4). As a result, they can be readily reused to execute other (sub)tasks that require the same alignment primitives. The subtasks are implemented as states in an FSM, with discrete monitors coordinating the overall execution (Fig. 5). It consists of following states and transitions:

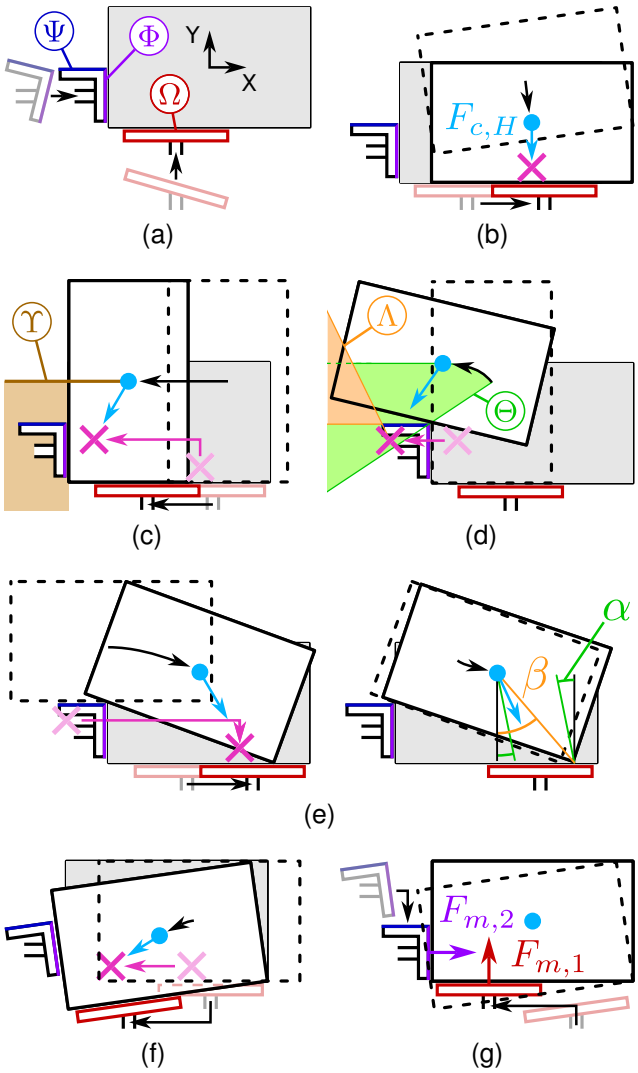


Fig. 4. Top-down view of the subtasks used in the stacking skill. The current pose of the payload is given by the white rectangle, its previous pose by the dashed outline. The object is depicted with the grey rectangle. The crane position above the frame is given by ✕, magenta arrows depict its movement; the cable attachment position is shown with ●, and the horizontal component of the cable force $F_{c,H}$ is shown by the cyan arrow. (a) ***Touch-object***. (b) ***Collide-payload***. (c) & (d) ***Rotate-payload***. (e) ***Collide-payload*** after ***rotate-payload***. The friction angle is given by α, and is also projected to ●. (f) ***Place-payload***. (g) ***Align-payload***.

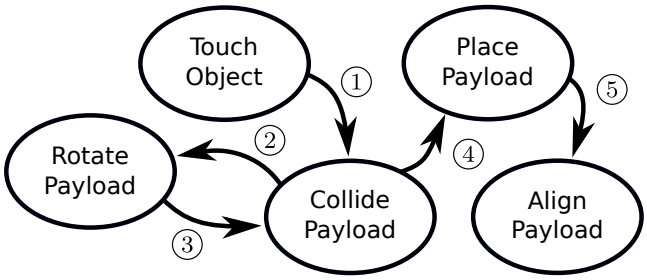


Fig. 5. Finite state machine used to coordinates the subtasks of Fig. 4.

1) ***Touch-object****:* This state aligns both end-effectors with both sides of the closest corner of the object.

The end-effectors are controlled such that they move perpendicularly towards the object, aligning Φ and Ω (Fig. 4a).

During this motion, the force at the end-effector is estimated.

Once a sudden variation in this estimation is detected for both end-effectors, the exact position of the object is localised, and state transition ① triggers.

2) ***Collide-payload****:* This state aligns a non-specific side-face of the payload with Ω, which is aligned with the object.

First, the manipulator slides Ω along the object to a position such that an approaching payload will not collide with Ψ. A small force perpendicular to the object is applied, such that proper contact is maintained. Next, the crane (✕) lifts the payload up and moves to a position with a Y-value, such that the payload will collide any of its sides with Ω.

The horizontal component of the cable force $F_{c,H}$ ensures the payload remains in contact with Ω. It will either stabilise with its long side, or short side. Thus, the state uncertainty is mechanically reduced to two possibilities. Increasing the area of Ω makes this process more robust to variations of the crane position, and consequently on the direction of $F_{c,H}$.

When the orientation of the payload remains constant, it is aligned with the object. In case the wrong side is aligned, ④ triggers, otherwise ② activates.

3) ***Rotate-payload****:* This state performs a sequence of actions, aligning an unconstrained side of the payload with Φ (which is aligned with the object), before rotating the payload 90° to align this side with Ψ.

First, Φ slides along the object such that Ψ is within ϒ (Fig. 4c). Meanwhile, the crane moves to a position close to Φ. The flat end-effector follows the payload such that it is eventually constrained by both Ω and Φ into a corner.

Next, the crane moves with a constant X-velocity past Φ (Fig. 4d). Once ✕ is within Ω, $F_{c,H}$ will create a moment that causes the payload to rotate towards Ψ. The payload will slide and stabilise along Ψ, given that • is never within Λ, since this would result in a moment that rotates the payload past Ψ. Increasing the length of Ψ lowers this possibility. When the payload is rotated 90°, ③ triggers.

In the subsequent *collide-payload* state (Fig. 4e), both the crane and Ω move to the same position as before. Due to the cable force, the payload slides over Ψ and rotates such that its corner collides with Θ. In this configuration, the cable force should be both larger than the friction angle α, for the payload to slide and align with Θ; and smaller than β, such that it will not topple over to its wrong side. This behaviour can be monitored with the change of the payload pose.

4) ***Place-payload****:* This state aligns a corner of the payload with Θ and Ψ, before placing it on top of the object.

The crane is positioned such that the payload remains in contact with Θ and Ψ, due to the horizontal component of the cable force $F_{c,H}$, constraining two sides of the payload. If the top of the end-effector is below •, the reaction force R_G causes the payload to experience a moment, resulting in a non-zero pitch angle (Fig. 6). In the static case, this will be compensated by a counter-moment due to the weight of the payload F_G and the leverage arm d_G. Thus, when lowering the payload, the corner of the payload first making contact with the object will be in front of the end-effector. This causes the final placement position to be a distance d_H in front of end-effector. To compensate, the end-effectors are moved a distance $d_m > d_H$ away from the object before unreeling the cable. This results in the payload being placed slightly in front of the object, triggering ⑤. The resulting alignment error $d_m - d_H$ will be compensated by pushing the payload until it is aligned with the object.

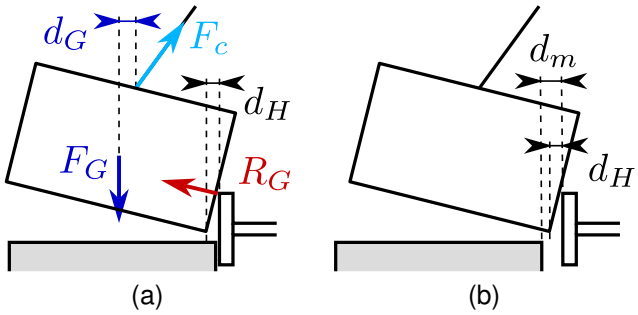


Fig. 6. (a) The reaction force R_G causes the payload to tilt, resulting in a placement past the constrained face when lowered. (b) The end-effector is moved a distance $d_m > d_H$, resulting in a placement in front of this face.

5) ***Align-payload****:* This state aligns the sides of the payload and the object. During this alignment, the bottom of the payload remains in contact with the top of the object.

The end-effectors are positioned in front of their respective side of the object. Then, they perform the follow sequence of motions one-by-one: First, the end-effector moves perpendicularly towards the object, pushing the payload, before colliding with the object. Next, the end-effector slides along the object, while maintaining a perpendicular force ($F_{m,1}$ or $F_{m,2}$), aligning the sides of the payload and the object.

After both end-effectors have performed this motion, the payload is stacked right on top of the object.

V. EXPERIMENTAL RESULTS AND DISCUSSION

To validate the control strategy, a use case was performed where a crate is stacked on top of a static crate with an overhead gantry crane and the manipulator discussed in III. This static crate acts as *'the object'* that provides mechanical constraints. A camera mounted on the gantry provides a top-down view and is used to track the horizontal position and orientation of the payload. The payload is already grasped at the start of the experiment. A possible implementation to grasp the payload is discussed in [2].

The manipulator was positioned in front of the object such that its flat- and L end-effector could each reach one side of the closest corner of the object. It was made sure that when the payload collides with Ω during the initial *collide-payload* state, it stabilises along its wrong side. Thus, the system is required to rotate the payload in order to stack it. Snapshots of the experiment are shown in Fig. 7.

The experiment was performed once with 'nominal' crane position setpoints for the *collide-payload*, *rotate-payload*, and *place-payload* states, that were experimentally determined. The corresponding position of both end-effectors of the manipulator are given in Fig. 8 (with respect to the frame defined in Fig. 4a).

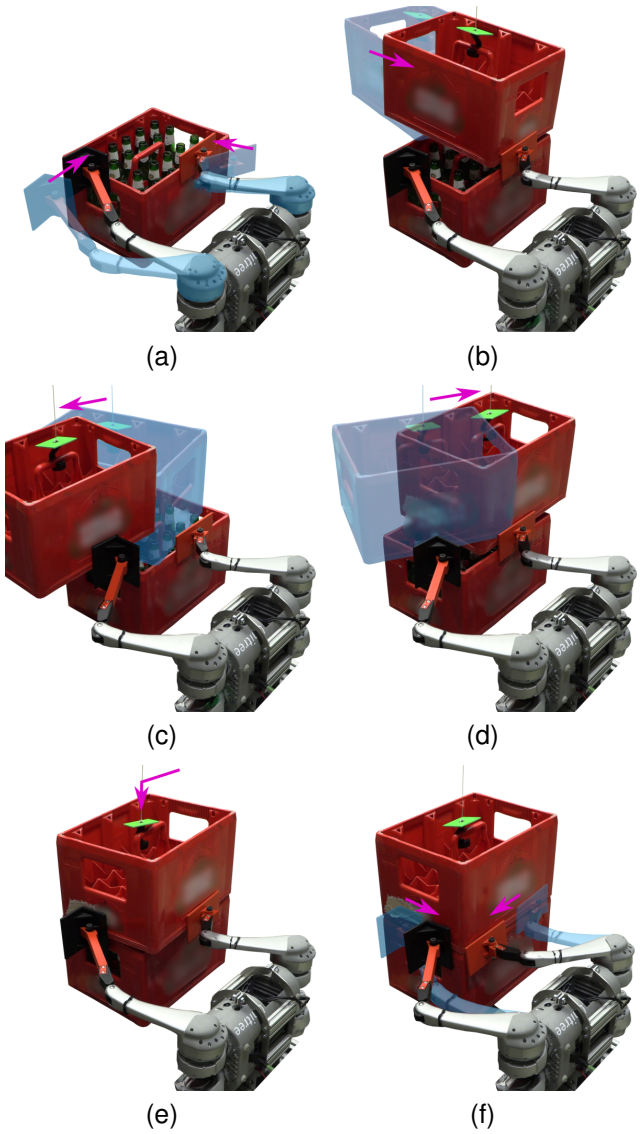


Fig. 7. Snapshots of the crate stacking experiments [15]. Previous positions of the payload and the manipulator are marked in transparent blue. The motions of the manipulator and the crane are given with magenta arrows. (a) ***Touch-object***. (b) ***Collide-payload***. (c) ***Rotate-payload***. (d) ***Collide-payload*** after ***rotate-payload***. (e) ***Place-payload***. (f) ***Align-payload***.

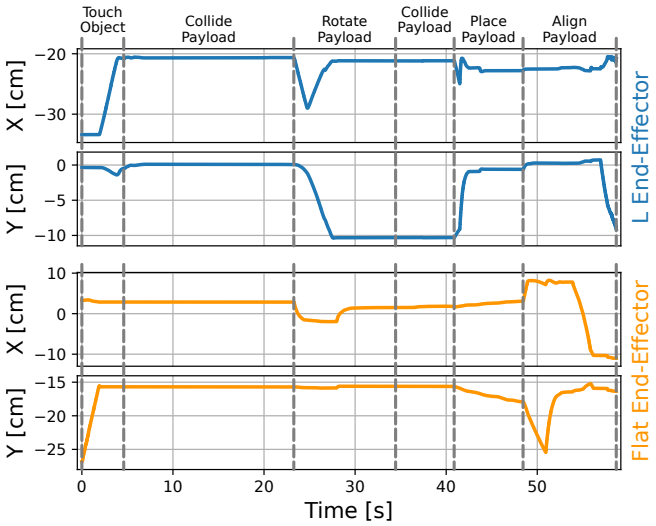


Fig. 8. Position of the flat and L end-effector of the manipulator.

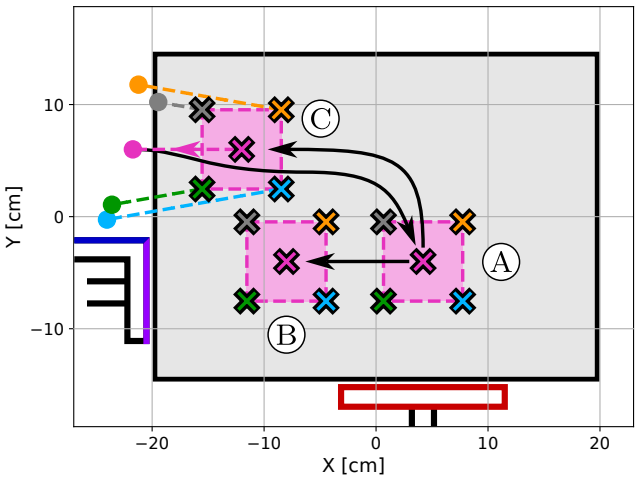


Fig. 9. Top-down view of the gantry positions during the execution. The positions at the end of the *collide-payload* and *place-payload* states are given by ✕ within ▢ for Ⓐ and Ⓑ respectively. The position setpoints during the first half of the *rotate-payload* state (corresponding to Fig. 4c) are indicated by Ⓒ. The constant velocity trajectory afterwards (Fig. 4d) is given with dashed lines. Monitor ③ triggered at the positions indicated with ●. The trial with the nominal setpoints is given in magenta. The other colours represent the trials with the manually added errors. The position of the object is highlighted in grey. Both end-effectors are marked at their respective side for reference. Their scale and position are only indicative.

Four additional trials were performed with manually added tracking errors. This simulates non-precise crane control, as is the case for cranes that are manually operated, which typically only feature an 'ON/OFF' control interface. For these trials, an error of 5cm was superimposed on the position of the nominal setpoints in different directions, each spaced out 90° from each other. In addition, during the second phase of the *rotate-payload* state (Fig. 4d), an angular error of 10° was introduced to the desired velocity direction of the crane. An overview of the crane positions and their variability during these states is given in Fig. 9.

For all trials, the system was able to detect during the initial *collide-payload* state that the payload was stabilised along its wrong side. This prompted the *rotate-payload* state, which successfully rotated the payload. During the subsequent *collide-payload* state, the payload slid over the end-effectors, stabilising along the desired side. After the following *place-payload* and *align-payload* states, the payload was positioned right on top of the object, successfully completing the box stacking. This showcases the robustness of the proposed approach against errors on the positioning and velocity direction of the crane.

The motion of the payload is almost entirely determined by its geometric relation with the mechanical constraints, created by the end-effectors of the manipulator. The execution will be successful given that the motion of the crane is within specific regions determined by this geometry. This can significantly limit the tracking requirements of the low-level controller of the crane, allowing the use of traditional, imprecise cranes. Only the friction forces are unknowns that

can influence the motion of the payload. However, their general direction remains predictable. Thus, their influence can be compensated by handling a conservative margin within these geometric regions.

It was not attempted to optimise the duration of the task execution in this work. Increasing the maximum velocity of the motion profiles, taking into account the payload- and collision dynamics and their mechanical bandwidth, would result in a faster execution.

The control and coordination between the crane and the manipulator of the current implementation occurs in open loop. Both agents perform their respective motions for the given subtask independent of each other. Allowing the agents to reactively adjust their control input based on sensory feedback of the other agent could improve the robustness of the implementation, the total execution time, and the possible manipulation actions. The trade-off is a more complex coordination, and a possibility to excite vibrations and unstable behaviours if the agents are not properly tuned to each other. A leader-follower approach (with a respective low- and high control bandwidth) could limit these trade-offs.

It should be noted that the used crates have mechanical features at their underside, designed such that they are easily stackable. This significantly assists the aligning process (similar features are used for other crates/bins used in logistics). The sliding motion during the *align-payload* state is less predictable for objects without these features, due to the complex friction effects. Deciding how and where to push to cause a specific motion is an active research domain [16].

Alternatively, other fine-positioning strategies can be performed to achieve the same result. For example, one end-effector can reach around and align itself with the side opposite of the one being pushed. This creates a mechanical brace against which the payload can be pushed and aligned (similar to the current *collide-payload* state). This process can be iterated across the different sides that need to be aligned until the required accuracy is reached. In certain scenarios, this brace feature can originate directly from the environment, e.g. a previously placed brick on the current masonry layer. Due to its limited workspace, this approach could not be implemented with the used manipulator.

VI. CONCLUSION

This paper proposed a multi-robot system, consisting of a crane and a dual-arm manipulator. It discussed the design of this manipulator to improve the control over a payload suspended by the crane. The end-effectors of the manipulator are designed to interact with the existing environment and create additional mechanical constraints at well-chosen positions. Passive joints and a specific mechanical design are used such that the end-effectors self-align when they perpendicularly collide with a surface. This eliminates the need for additional actuation, and its active control.

A coordinated control strategy between the manipulator and the crane was implemented to accurately position and stack crates. This approach exploits collisions and mechanical constraints to reduce the uncertainty of the payload orientation to two possible, stable states. The resulting state could be autonomously detected, and if needed, altered through a rotation skill, which mainly depends on the geometric relations between the system and the payload.

Trials with manually added setpoint errors could still successfully complete the task. This shows that accurate crane control is not necessary, since the behaviour of the payload is mainly determined by the mechanical constraints, highlighting the robustness of the solution. Thus, existing, imprecise cranes can be used during the execution, lowering the implementation barrier for real-life scenarios.

Future work will focus on an automated solution that can place entire layers in construction or palletising applications. Similar skills can be used to orient and position subsequent payloads next to previously placed payloads. The manipulator will also need to autonomously reposition itself.

REFERENCES

[1] "Jak budować w systemie Silka Tempo - film instruktażowy.," YouTube, uploaded by Ytong Silka Multipor, 21 February 2019, https://www.youtube.com/watch?v=j9KGIGf9HIQ.

[2] B. Deroo, E. Aertbelën, W. Decré and H. Bruyninckx, "Mechatronic Design and Control of a Robotized Crane Exploiting Natural Dynamics for Pick-and-Place Applications," IEEE Trans. on Robotics, vol. 42, pp. 782-798, 2026.

[3] M. Gouttefarde, J. -F. Collard, N. Riehl and C. Baradat, "Geometry Selection of a Redundantly Actuated Cable-Suspended Parallel Robot," IEEE Trans. on Robotics, vol. 31, no. 2, pp. 501-510, April 2015.

[4] A. Pott et al., "Cable-driven parallel robots for industrial applications: The IPAnema system family," IEEE ISR 2013, Seoul, Korea (South), pp. 1-6, 2013.

[5] T. Bruckmann, R. Boumann, "Simulation and optimization of automated masonry construction using cable robots," Advanced Engineering Informatics, vol. 50, pp. 101388, 2021.

[6] D Liu, J. Yi, D. Zhao, W. Wang, "Adaptive sliding mode fuzzy control for a two-dimensional overhead crane," Mechatronics, vol. 15, no. 5, pp. 505-522, 2005.

[7] N. C. Singer and W. P. Seering, "Preshaping Command Inputs to Reduce System Vibration," ASME. Journal of Dynamic Systems, Measurement, and Control, vol. 112, no. 1, pp.76-82, March 1990.

[8] M. Ambrosino, F. Boucher, P. Mengeot, E. Garone, "Experimental validation of a constrained control architecture for a multi-robot bricklayer system," Mechatronics, vol. 98, pp. 103139, 2024.

[9] P. M. Wensing, et al., "Proprioceptive Actuator Design in the MIT Cheetah: Impact Mitigation and High-Bandwidth Physical Interaction for Dynamic Legged Robots," IEEE Trans. on Robotics, vol. 33, no. 3, pp. 509-522, June 2017.

[10] B. Pousett, J. Ubbink, W. Decré and H. Bruyninckx, "Collaborative Block Stacking with Non-Prehensile Catching," Int. Symp. on Automation and Robotics in Construction (ISARC), 2026.

[11] M. A. Erdmann and M. T. Mason, "An exploration of sensorless manipulation," IEEE Journal on Robotics and Automation, vol. 4, no. 4, pp. 369-379, Aug. 1988.

[12] I. M. Bullock, R. R. Ma and A. M. Dollar, "A Hand-Centric Classification of Human and Robot Dexterous Manipulation," IEEE Trans. on Haptics, vol. 6, no. 2, pp. 129-144, April-June 2013.

[13] N. Chavan-Dafle and A. Rodriguez, "Prehensile pushing: In-hand manipulation with push-primitives," 2015 IEEE/RSJ Int. Conf. on Intelligent Robots and Systems (IROS), pp. 6215-6222, 2015.

[14] B. Pousett, B. Deroo, W. Decré and H. Bruyninckx, "Conversion of a Quadruped to Low-Cost, Multi-Arm Manipulator," Benelux Meeting on Systems and Control, 2024.

[15] "A Multi-Robot Hoisting System that Achieves Precision by Exploiting Mechanical Constraints," YouTube, uploaded by Robotics Research Group, KU Leuven, 29 May 2026, https://www.youtube.com/watch?v=T7Dz6usEDIY.

[16] F. R. Hogan and A. Rodriguez, "Feedback control of the pusher-slider system: A story of hybrid and underactuated contact dynamics," Algorithmic Foundations of Robotics XII, pp. 800–815, Springer, 2020.